BIOMECHANICAL MODEL USING MULTIBODY DYNAMICS FOR HUMAN BODY IMPACT

Jorge A. C. Ambrósio
Instituto de Engenharia Mecânica, Instituto Superior Técnico, Lisboa, Portugal

INTRODUCTION

Models for the simulation of sports activities with body impact draw many of their features from the use of multibody dynamics. The efficiency and accuracy of the numerical procedures for the simulation of the human body is of utmost importance. The model must describe precisely the relative range of motion of the different segments of the human body, the forces transmitted between them and the impact/contact that involve biomechanical components.

Several formulations based on the use of different sets of coordinates can be found in the literature to derive automatically the equations of motion for a general multibody system. Using the concept of pseudo-velocities Kane (1985) describes the multibody motion by a minimal set of variables when open-loop systems are modelled. However, it is not always clear the physical meaning of variables used. On the other hand, the use of Cartesian coordinates correspond to one of the most popular methodologies to describe spatial multibody systems (Nikravesh, 1988; Haug, 1989). The coordinates are the position and spatial orientation of each of the system components, described in terms of local reference frames fixed to the moving bodies. In orther to avoid the use of rotational coordinates (Euler angles, Euler parameters, Bryant angles, etc.) Jalón (1994) proposes the use of a set of coordinates, known as natural coordinates, composed by the positions of points and vectors in an inertial reference frame. Though these coordinates give raise to a much larger set of equations to describe the same system the nonlinearity of the equations of motion is much smaller than what is obtained with other formulations. The numerical problems associated with the use of large sets of coordinates is solved by transforming the equations of motion from dependent to independent using velocity transformations (Jerkovsky, 1978; Nikravesh and Gim, 1989). The final set of equations of motion obtained is much smaller than with the methods referred. However, some computational costs are associated with the use of the transformations.

Claims for better performance of one methodology relative to another are very often application dependent and consequently are not discussed here. Regardless of the formulation selected it is always possible to recover the reaction forces between the system components, in particular in biomechanical applications, the forces exerted between different body segments. Based on a general methodology using natural coordinates (Jalon, 1994), a whole body response model is presented in this work. The joints between biomechanical segments are defined by forcing adjacent bodies to share common points and vectors. A better efficiency in the integration of the equations of motion is obtained using an augmented Lagrange formulation (Bayo, 1996).

Regardless of the formulation used to describe the motion of the biomechanical model, it is necessary to describe the forces resulting from contact situations with other objects or anatomical segments of the multibody system. The collision or contact between two bodies is characterised by forces that develop and disappear over a short period of time. The physics of the contact

and the relation between geometry and material properties of the surfaces must be described while the force model should not disrupt the stability of the numerical integration of the equations of motion. A classical approach to solve this problem as a discontinuous event is based on the momentum balance impulse equations. This methodology provides the velocity jump that results from a collision (Wehage, 1980; Lankarani and Nikravesh, 1992). Alternatively, local deformations and contact forces are treated as continuous events and introduced in the system equations of motion. A model proposed, by Lankarani and Nikravesh (1990) based on the Hertzlan contact theory (Hertz, 1895), includes energy dissipation due to localized deformation effects is extensively used here to model impact/contact between the components of the biomechanical model.

In the definition of the joints between the biomechanical segments no considerations are generally made with respect to their feasible range of motion. In this model realistic limits on the relative range of motion between body segments are obtained introducing a set of articular penalty forces in the model rather than setting up new unilateral constraints between the system components. These forces representing the reaction moments between the body segments are activated when the biomechanical joints reach the limit of their range of motion and prevent the model from achieving physically unacceptable positions (CIBA, 1979). This is a problem of intermittent motion that forces high frequency components of the system response to appear. Improved efficiency in the integration process of the equations of motion is obtained by modeling the penalty forces with a continuous contact-impact force model including energy dissipation as in the case of body impact (Lankarani and Menon, 1995).

The biomechanical model developed is composed of 12 rigid bodies and it is suitable for application to individuals with different sizes. Its application is illustrated with the simulations of an automobile occupant during a crash and the impact of an athlete in a sports scenario. Based on the results obtained the methodology is discussed and conclusions are drawn.

FORMULATION OF THE EQUATIONS OF MOTION

A multibody system is a collection of rigid and/or flexible bodies with their relative motion constrained by kinematic joints and acted by external and/or internal forces, as depicted by figure 1. Depending on the application of the system it may be necessary to model some of the system components as flexible bodies. In biomechanical applications, that is the case of models for the simulation of aircraft crash scenarios where the flexibility of the neck and spine play an important role. For the purpose of this work issues concerning with the flexibility of the biomechanical components are not discussed. The interested reader is referred to the reference (Pereira and Ambrósio, 1994).

Different sets of coordinates can be used to formulate the equations of motion of the biomechanical model. All the formulations, regardless of the set of coordinates used, allow for the calculation of loads transmitted between the anatomical segments of the human body. However, when other considerations, such as the partition of the intersegmental forces between muscle actions and joint reactions, take place the problem becomes more complex (Winter, 1990; Berme et al., 1987). The cases considered in this paper do not involve active muscle actions and consequently the problems associated with the calculation of the forces for redundant systems will not be considered here.
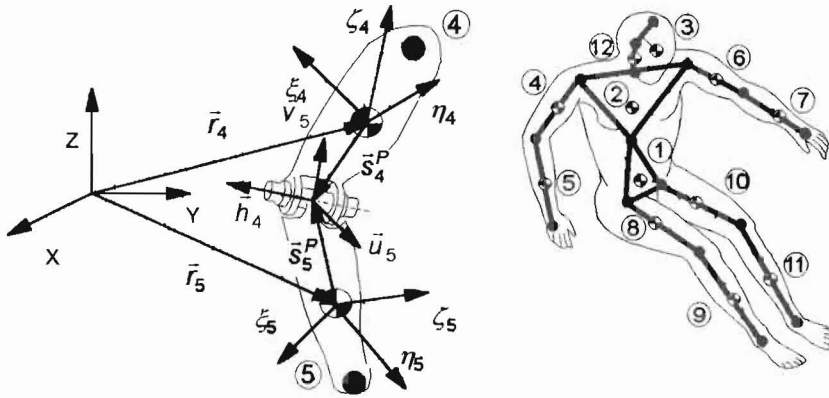
Figure 1 - Three-dimensional biomechanical model and a typical joint

In the modelling problems considered in this work all the anatomical joints are modelled as mechanical joints. Though this is appropriate as a first order approximation for a wide variety of applications, such as those considered here, a more detailed joint modelling may be necessary for application in gait and performance analysis.

Cartesian Coordinates

The position and orientation of each component of the biomechanical model is described by a position vector r_i and a set of rotational coordinates p_i (Nikravesh, 1988). The kinematic constraint illustrated in figure 1 is represented by a set of five equations given by:

$$\Phi^{(\text{rev})} \equiv \left\{ \begin{array}{c} \mathbf{r}_4 + \mathbf{s}_4^P - \mathbf{r}_5 - \mathbf{s}_5^P \\ \mathbf{h}_4^T \mathbf{v}_5 \\ \mathbf{h}_4^T \mathbf{u}_5 \end{array} \right\} = \mathbf{0} \tag{1}$$

where the first three equations represent that bodies 4 and 5 share the same point P and the remaining two equations state that two points in each body, along the relative axis of rotation, have to be parallel all the time. Similar equations are derived for the rest of the joints of the system. The second time derivative of equation (1) gives raise to the acceleration equations written as

$$\Phi_q \ddot{\mathbf{q}} = -\frac{\partial^2 \Phi}{\partial t^2} - \frac{\partial}{\partial t}\left(\Phi_q\right)\dot{\mathbf{q}} \tag{2}$$

where Φ_q denotes the Jacobian matrix. The equations of motion for a single rigid body i are given by

$$m_i \ddot{\mathbf{r}}_i = \mathbf{f}_i$$
$$\mathbf{J}_i' \dot{\omega}_i' = \mathbf{n}_i' - \tilde{\omega}_i' \mathbf{J}_i' \omega_i' \tag{3}$$

where $\mathbf{f}_i$ is the resultant of the applied forces, $\mathbf{n}_i$ is the sum of the moments applied directly to body i or resulting from forces not applied in the body fixed referential origin, m is the body mass and $\mathbf{J}$ is its inertia tensor. Quantities with a prime $(.)'$ mean that they are expressed in body fixed coordinates. Equation (3) is

39

evaluated for all bodies in the system, while the forces are also calculated for all components. This is written in a matrix form as

$$M\ddot{q} = g \tag{4}$$

where vector g contains all applied forces, moments and the gyroscopic forces.

The kinematic constraints are added to the equations of motion of the unconstrained system described by equation (4) using the Lagrange multiplier technique (Nikravesh, 1988). Defining by λ the vector of unknown Lagrange multipliers the equations of motion of the constrained system are written as a system of differential and algebraic equations described by

$$\begin{bmatrix} M & \Phi_q^T \\ \Phi_q & 0 \end{bmatrix} \begin{bmatrix} \ddot{q} \\ \lambda \end{bmatrix} = \begin{bmatrix} g \\ -\dfrac{\partial^2 \Phi}{\partial t^2} - \dfrac{\partial}{\partial t}(\Phi_q)\dot{q} \end{bmatrix} \tag{5}$$

The forces transmitted between the different segments of the system are related with the vector of Lagrange multipliers and the Jacobian matrix as

$$f_r = -\Phi_q^T \lambda \tag{6}$$

All intersegmental forces and contact forces are evaluated and introduced in vector g for each time step. Equation (5) is then used to calculate the system accelerations and these are integrated together with the velocities to calculate the new velocities and positions. The procedure proceeds until the complete motion of the system is obtained in the time interval.

Natural Coordinates

Alternatively to the Cartesian coordinates a set of natural coordinates are used to evaluate the equations of motion of the system. The idea is to describe a body by a collection of points and vectors, such as the body presented in figure 2, which is defined by two basic points and two non-coplanar unit vectors. It can be shown other rigid bodies may be derived from this basic body by means of a coordinate transformation (Jalon, 1994).
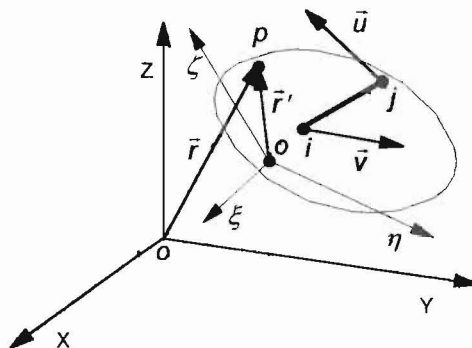

Figure 2 - Inertial and local system of coordinates.

Let the rigid body have a local reference frame (ξ, η, ζ) rigidly attach to it and with origin located in point o, which is not necessarily its centre of mass. The principle of the virtual power is used to derive the equations of motion of a rigid

40

body. For this purpose the position vector **r** is described as a function of the basic points and vectors of the rigid body as:

$$\mathbf{r} = \mathbf{C}\mathbf{q}_e \tag{7}$$

where **C** is a transformation matrix, that is independent of the motion of the body and therefore constant in time and $\mathbf{q}_e$ are the coordinates of the basic points and vectors. Differentiating equation (7) twice in respect to time provides the velocity and acceleration of point P are obtained as:

$$\dot{\mathbf{r}} = \mathbf{C}\dot{\mathbf{q}}_e \tag{8}$$

$$\ddot{\mathbf{r}} = \mathbf{C}\ddot{\mathbf{q}}_e \tag{9}$$

The virtual power of the inertia forces for the rigid body is expressed as:

$$W^* = -\dot{\mathbf{q}}_e^{*^T}\left(\rho\int_\Omega \mathbf{C}^T\mathbf{C}\ d\Omega\right)\ddot{\mathbf{q}}_e \tag{10}$$

where ρ is the mass density and Ω the volume of the rigid body. It must be noted that virtual velocity vector $\dot{\mathbf{q}}_e^*$ and the acceleration vector for the basic vectors and points $\ddot{\mathbf{q}}_e$ are independent of the body volume. The body mass matrix is

$$\mathbf{M} = \rho\int_\Omega \mathbf{C}^T\mathbf{C}\ d\Omega \tag{11}$$

The mass matrix of bodies defined with different sets of basic points and vectors is obtained from this matrix after a proper coordinate transformation.

Concentrated forces can be applied in a generic point of the rigid body, other than a basic point, as described by figure 3(a). The case of an applied moment, as depicted by figure 3(b), is described by a force binary where the two opposite forces act in a plane perpendicular to the applied moment.
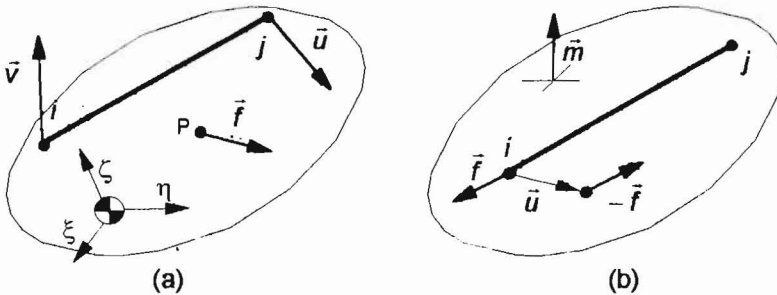

Figure 3 Applied forces and moments: (a) External force; (b) Applied moment

The concentrated force $\mathbf{f}_P$ applied on point P of a rigid body is described by a generalized force $\mathbf{g}_e$, applied to the basic points and vectors of that body. The relation between these forces is described by the virtual work given by

$$\delta W = \delta\mathbf{r}_p^T\mathbf{f}_p = \delta\mathbf{q}_e^T\mathbf{g}_e \tag{12}$$

Vector $\mathbf{r}_p$, representing the position of point P, is related with the basic coordinates by equation (7). Comparing the terms of the resulting equations, it is found that:

$$\mathbf{g}_e = \mathbf{C}_p^T\mathbf{f}_p \tag{13}$$

An applied moment is described here by a torque **m** given by two non-collinear and opposite forces **f** related by

$$\mathbf{m} = \tilde{\mathbf{u}}_m \mathbf{f}_m \tag{13}$$

where **u** is a unit vector given by:

$$\mathbf{u}_m = -\frac{\tilde{\mathbf{m}}(\mathbf{r}_j - \mathbf{r}_i)}{\|\tilde{\mathbf{m}}(\mathbf{r}_j - \mathbf{r}_i)\|} \tag{14}$$

after some algebraic manipulations it is found that the generalized force describing the applied moment is written as (Jalon, 1994)

$$\mathbf{g}_e = (\mathbf{C}_i^T + \mathbf{C}_{i+u_m}^T)\mathbf{f}_m \tag{15}$$

In order for the set of coordinates with the positions of the basic points and vectors to represent a rigid body some kinematic constraints must be imposed. Relating to figure 4, the kinematic constraints that describe the conditions of constant vector length and constant angle are illustrated as

$$\Phi^{(cd,1)} = (\mathbf{r}_j - \mathbf{r}_i)^T(\mathbf{r}_j - \mathbf{r}_i) - L_{ij}^2 = 0 \tag{16}$$

$$\Phi^{(a2v,1)} \equiv \mathbf{u}_i^T \mathbf{u}_j - \cos(\alpha) = 0 \tag{17}$$

where the condition of a constant angle between **u** and **v** and a constant distance between points i and j was used. Equations (16) are evaluated for all constraints in the multibody system and added to the equations of motion of the system components. The constrained equations of motion are written in a form similar to equation (5) and solved using the augmented Lagrangean method (Bayo, 1996).

CONTACT/IMPACT FORCE MODEL
In order to have a reliable model for the contact/impact of the human body special care has to be given to the numerical description of the contact forces. The model must include the contact speed and compliance in a form that is related to the geometry and material properties of the bodies in contact. Moreover, the contact force model must be suitable for a stable integration of the biomechanical model equations of motion. These characteristics are obtained with a continuous contact force model (Lankarani and Nikravesh, 1990).

Let the contact force between a segment of the biomechanical model and a surface of an object or another segment be a function of a pseudo penetration and a pseudo velocity of penetration given by

$$\mathbf{f}_{s,j} = \left(K\delta^n + D\dot{\delta}\right)\mathbf{u} \tag{18}$$

where D is a damping coefficient and K is a generalized stiffness coefficient which
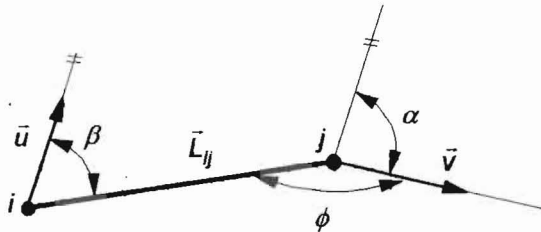

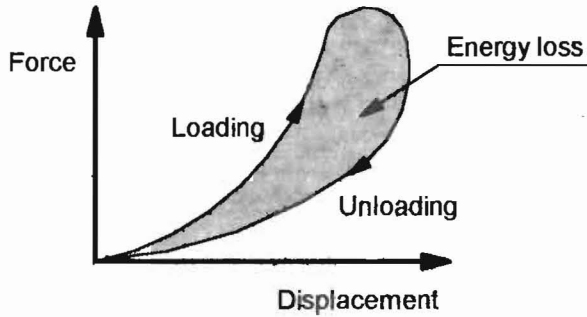Figure 4 Kinematic constraints defining a rigid body

Figure 5. Force displacement relationship accounting for hysteresis

depends on the geometry of the surfaces in contact and their material properties. The damping coefficient, which introduces the hysteresis damping for the surfaces in contact, as depicted by figure 5, can be shown to be a function of impact velocity $\dot{\delta}^{(-)}$, relative stiffness of the contacting surfaces and restitution coefficient e. The contact force is finally given by

$$\mathbf{f}_{s,i} = K\delta^n\left[1 + \frac{3(1-e^2)}{4}\frac{\dot{\delta}}{\dot{\delta}^{(-)}}\right]\mathbf{u} \tag{19}$$

Note that the restitution coefficient e reflects the type of impact (for a fully elastic contact $e=1$ while for a fully plastic contact $e=0$). This equation is valid for impact velocities lower than the propagation speed of elastic waves across the bodies, i.e., $\dot{\delta}^{(-)} \leq 10^{-5}\sqrt{E/\rho}$. In all applications considered here this criterion is fulfilled.

BIOMECHANICAL MODEL

Using the methodology discussed previously it is presented here a three-dimensional, whole body response, biomechanical model of the human body suitable for impact simulations. The model is general and accepts data for any individual. The information required to assemble the equations of motion of the model includes the mass and inertia of the biomechanical segments, their lengths, location of the body-fixed coordinate frames and the geometry of the potential contact surfaces, as pictured in figure 6. The data hold within the database can be expanded for different individuals. For this work, the data available concerns the models of a 50% anthropomorphic dummy used for human contact modelling during crash of transportation systems and of a 50% human male. It is not the intention of this work to discuss the different databases or measuring techniques used to collect data necessary for the construction of any particular biomechanical model. The interested reader is referred to Nigg and Herzog (1994).

In contact/impact simulations the relative kinematics of the head-neck and torso are important to the correct evaluation of the loads transmitted to the human body. Consequently, the head and neck are modelled as separate bodies and the torso is divided in two bodies. The hands and feet do not play a significant role in this type of problems. They are included in the lower arms and legs respectively.

43

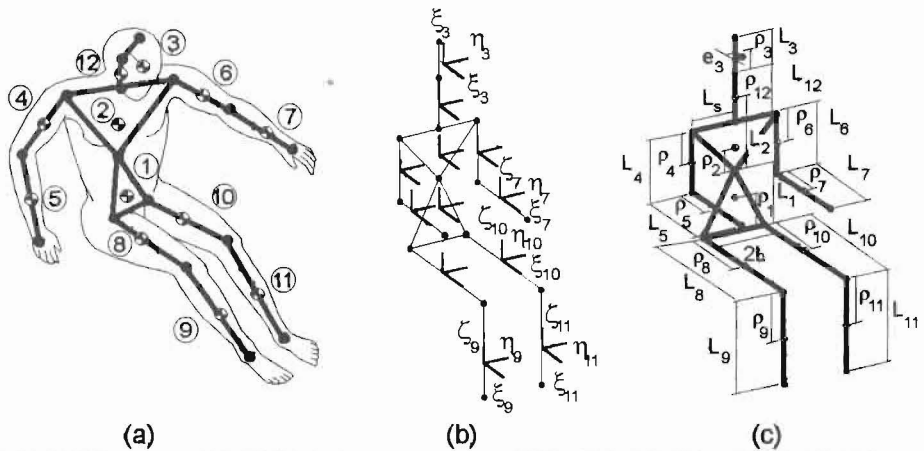(a)   (b)   (c)

Figure 6 Three-dimensional biomechanical model for impact: (a) actual model;
(b) local referential locations; (c) dimensions for the segments.

The model is described using twelve rigid bodies defined using sixteen
basic points and seventeen unit vectors located at the articulations and
extremities. A total of ninety-nine natural coordinates are created. Seventy
kinematic constraints are used in the definition of the rigid bodies. The result is a
biomechanical model with twenty-nine degrees of freedom. In table 1, the
description and location of the eleven kinematic joints is presented.

Table 1 -Kinematic joint description for biomechanical model.

Joint	Type	Description
1	spherical	Back, (12th thoracic and 1st lumbar vertebrae).
2	spherical	Torso-Neck (7th cervical and 1st thoracic vertebrae).
3-5	spherical	Shoulder.
4-6	revolute	Elbow.
7-9	spherical	Hip.
8-10	revolute	Knee.
11	revolute	Head-Neck, (at occipital condyles).

The principal dimensions of the model are represented in figure 6 (c). In
most cases, the effective link-lengths between two kinematic joints is used instead
of standard anthropometric dimensions based on external measurements. The set
of data concerned with the models referred are described in (Laananen, 1983).

Joint resisting moments

In the biomechanical model, no active muscle force is considered.
However, the muscle passive behaviour is represented by joint resistance
torques. Moreover, physically unacceptable positions of the body segments are
prevented by applying a set of penalty torques anytime that two segments of the
biomechanical model reach the limit of their relative range of motion. The joint
resistance torques are modelled using a viscous torsional damper and a non-
linear torsional spring, located in each kinematic joint.

44

Take the elbow of the model, represented in figure 7, as an example of a joint modelled by a revolute joint. Here the axis for the relative rotation of the lower and upper arm is represented. The torsional damper has a small constant coefficient j_i being the total damping torque at each joint given by

$$\mathbf{m}_{d_i} = -j_i \, \dot{\beta}_i \tag{20}$$

where $\dot{\beta}_i$ is the relative angular velocity vector between the two bodies interconnected by that joint and the index i denotes the joint number.
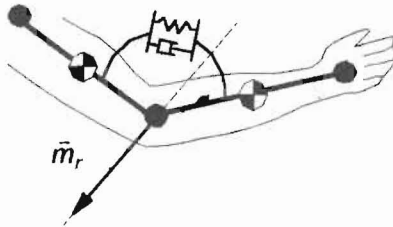
Figure 7   Joint resistance torque modelled using non-linear spring and damper.

The contribution of the non-linear spring has two terms. The first one is a resisting torque m_{ri} that acts to resist the motion of the joint. For the dummy joint, this torque has a constant value and its applied to the whole range of motion (Silva, 1996). For the human joint this torque has an initial value which drops to zero after a small angular displacement from the joint initial position. In both cases, this torque has a direction opposite to the direction of the relative angular velocity vector between the two bodies interconnected in that joint, this is

$$\mathbf{m}_{r_i} = -m_{r_i} \, \dot{\beta}_i \Big/ \left\| \dot{\beta}_i \right\| \tag{21}$$

The second term is a penalty resisting torque $\mathbf{m}_{pi}$. This torque is null during the normal joint rotation but it increases rapidly, from zero until it reaches a maximum value, when the two bodies interconnected by that joint, reach physically unacceptable positions. The curve for the penalty resisting moment is represented in figure 8 qualitatively.
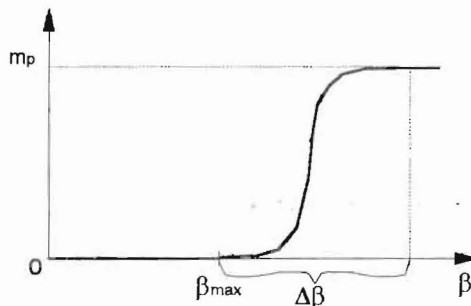

Figure 8   Penalty moment for the elbow.

The shoulder is an example of a biomechanical joint modelled by a spherical joint as depicted by figure 9. In order to calculate the penalty torque it is

45

necessary to construct the cone of feasible motion. This cone has its tip in the center of a sphere with a unit radius. While the upper arm moves inside the cone its motion does not imply any displacement of the upper or lower torso.
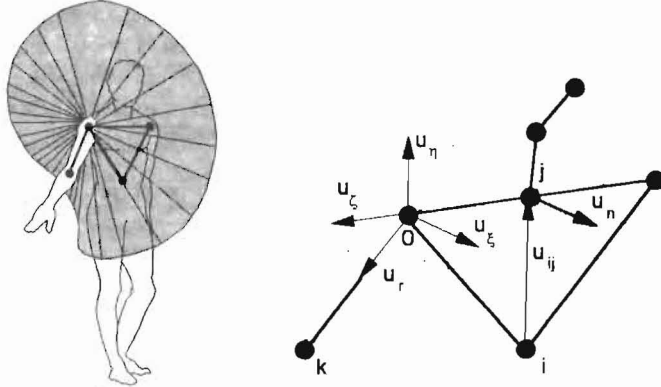

Figure 9 Cone of feasible motion for the shoulder joint.

A local reference frame is constructed and rigidly attached to the shoulder joint (points 3 and 5), as shown in figure 9. The vectors defining the local axes u_x and u_h are built using basic points and vectors of the upper torso

$$\mathbf{u}_\xi = \mathbf{u}_n \tag{22}$$

$$\mathbf{u}_\eta = \frac{\mathbf{r}_j - \mathbf{r}_l}{\|\mathbf{r}_j - \mathbf{r}_i\|} \tag{23}$$

A third base vector is calculated as the cross product of the first two:

$$\mathbf{u}_\zeta = \tilde{\mathbf{u}}_\xi \mathbf{u}_\eta \tag{24}$$

A fourth vector in the direction of the upper arm is calculated using the two basic points of this body

$$\mathbf{u}_r = \frac{\mathbf{r}_k - \mathbf{r}_o}{\|\mathbf{r}_k - \mathbf{r}_o\|} \tag{25}$$

With these vectors, the angles of longitude θ and latitude β of the unit vector $\mathbf{u}_r$ are calculated in the local reference frame, as depicted in figure 10(a). The angle of maximum amplitude β_{max} is also calculated for a specified longitude θ, using a cubic spline interpolation curve. This curve, uses the angles of maximum amplitude at the four main quadrants β_I, β_{II}, β_{III} and β_{IV}, to interpolate β_{max}, as shown in figure 10(b). If the effective latitude β is larger than the maximum latitude β_{max}, a penetration on a zone of unfeasible motion occurs and a penalty resisting torque is applied. The magnitude of this torque, in the direction of the cross-product between vector u_z and vector u_r, increases rapidly with the penetration. The penalty torque is given by

$$\mathbf{m}_{p_i} = m_{p_i} \left[3 \left(\frac{\beta_i - \beta_{i_{max}}}{\Delta \beta_i} \right)^2 - 2 \left(\frac{\beta_i - \beta_{i_{max}}}{\Delta \beta_i} \right)^3 \right] \tilde{\mathbf{u}}_\zeta \mathbf{u}_r \tag{26}$$
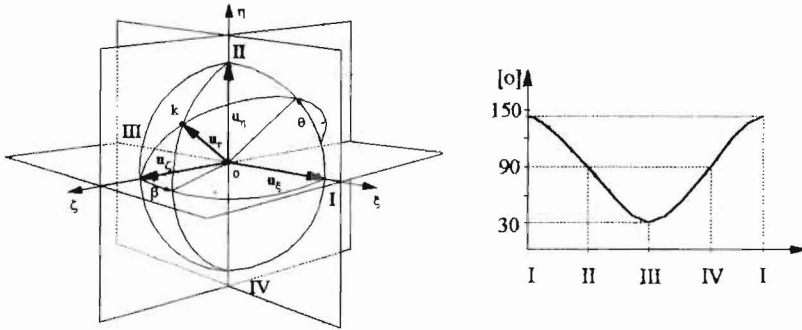
Figure 10 Angles and interpolation curve for the shoulder joint.

where the term between brackets is a third order polinomial with a behavior similar to that depicted by figure 8. Table 2 describes the values for the limit angles for different joints of the human body.

Table 2   Joint limit angles and force data.

Joint	$\beta_{i\ I}[°]$	$\beta_{i\ II}[°]$	$\beta_{i\ III}[°]$	$\beta_{i\ IV}[°]$	$\Delta\beta_i[°]$	$m_i[g]$	$m_{pi}[Nm]$	$j_i[Nms]$
1	40	35.0	30.0	35.0	11.5	2.0	226.0	16.95
2	60	40.0	60.0	40.0	15.0	2.0	678.0	3.39
3-5	140	90.0	30.0	90.0	11.5	1.0	226.0	3.76
4-6	90	-	45.0	-	11.5	1.0	226.0	3.39
7-9	10	120.0	50.0	45.0	11.5	2.0	452.0	5.65
8-10	-	90.0	-	45.0	11.5	1.0	226.0	5.65
11	19	-	2.0	-	15.0	2.0	452.0	16.95

Contact Surfaces

A set of contact surfaces is defined for the calculation of the external forces exerted on the model when the surfaces of the bodies contact other objects or different body segments. These surfaces are ellipsoids and cylinders with the form depicted by figure 11 and with the dimensions described in table 3.
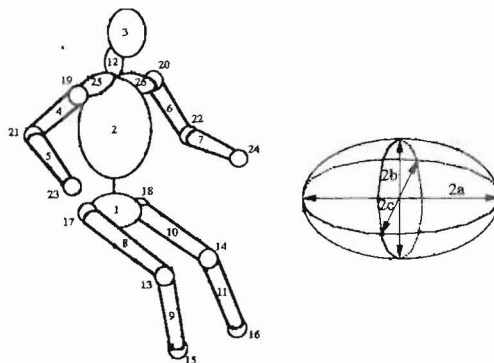

Figure 11 Representation of contact surfaces.

When contact between a component of the biomechanical model is detected a contact force, with the characteristics described by equation (19), is

47

applied to that component in the point of contact and with a direction normal to the surface. Friction forces are also applied to the contact surfaces using Coulomb friction. It must be noted that in general applications of the biomechanical model, now presented, it is important a characterisation of the surfaces in contact. Although in many cases this is a difficult task, even with incomplete data it is possible to obtain envelopes for the biomechanical response.

Table 3 - Dimensions of contact surfaces.

Body	50% Human Male $R_i[m]$	50% Anthropomorphic Dummy $R_i[m]$
1	0.102	0.114
2	0.127	0.114
3	0.095	0.0874
4 - 6	0.053	0.050
5 - 7	0.042	0.047
8 - 10	0.083	0.079
9 - 11	0.057	0.058
12	0.051	0.051

APPLICATION EXAMPLES

The biomechanical model described in this work is applied in different situations of human motion where activation of the muscle forces do not play a role. This is the case of unexpected contact of the human body. The cases of a car driver during a crash and a player during a unexpected tackle are simulated in order to demonstrate the methodology.

Car occupant during a crash

The case of a car occupant of a vehicle moving with a velocity of 20 Km/h towards a rigid barrier is simulated here. The model of a 50% human male is used for the simulation of the driver. The potential surfaces of contact with the occupant are the seat belts and the car seat, as pictured in figure 12. The vehicle has a structure, not shown here, that deforms during contact and dissipates the kinetic energy of the system.

The simulation shows that when the car impacts the rigid obstacle the occupant moves forward and stretches the seat belt. Due to the lack of symmetry of the shoulder belt the torso of the occupant has a rotation about the axis of the
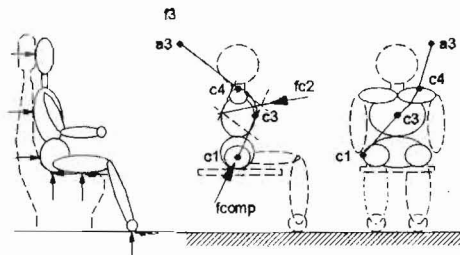

Figure 12   Forces on a car occupant due to the seat belt and the contact with the seat and car interior.
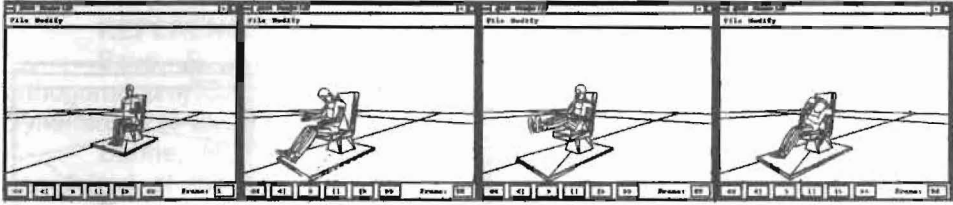
Figure 13 Motion of the occupant during the impact

spine while bending forward, as shown in figure 13. The head ,subjected to the accelerations pictured in figure 14, does not hit any surface modelled in the analysis. It is clear from figure 14 that the limit of motion between the neck and the upper torso is reached. After the impact the occupant retains the seated position in the car.
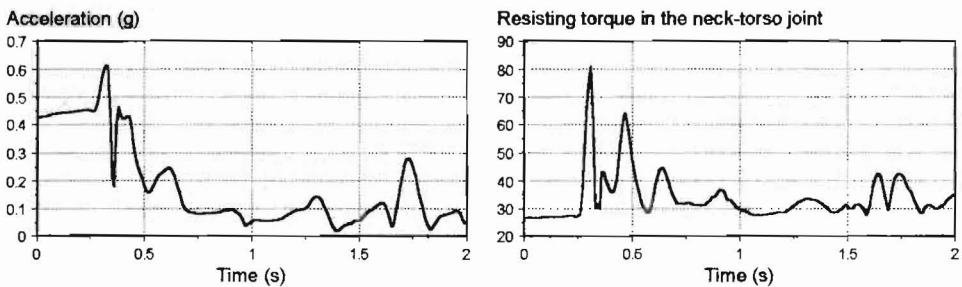

Figure 14 Acceleration of the occupant head and resisting torque on the joint between the neck and the upper-torso

Frontal tackle of an athlete

The human body can be subjected to impact in different athletic activities. Sports like rugby, American football or boxing exemplify some of the most visible cases of impact. Many executions in these sports are characterised by high impact loads in a short period of time without an active muscle reaction of the human subject. The case of a frontal tackle of a player by another player is simulated here to show the application of the presented methodology in a normal sports scenario. It must be noted that no special attention is paid in this simulation to issues related to the technical correctness of the tackle.

The player represented in figure 15(a) is hit by another player at the level of the lower torso. The incoming player has a mass of 75 Kg and is moving forward with a velocity of 3 m/s. The contact between the two players and between the standing player and the ground is modelled. The resulting motion is presented in figure 15.

From the results of the simulation it is observed that the head of the player hits the ground 0.63 s, after the impact between the players, reaching an acceleration of 1.2 g. The contact between the shoulders and the ground occurs at the same time, as displayed in figure 16. Based on the compliance of the surfaces in contact and any protective equipment, conclusions can be drawn on how the athlete withstands the impact and on the potential for injury.
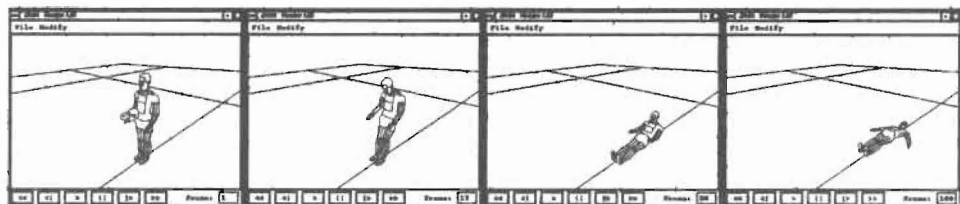
49

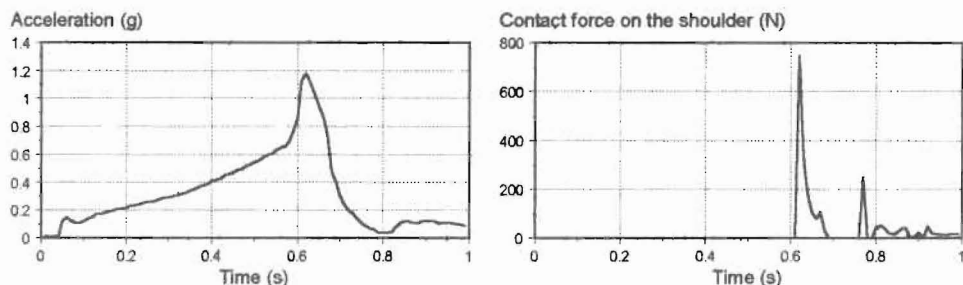Figure 15 Motion of the athlete during the tackle

Figure 16 Head Acceleration and contact force on the shoulder

CONCLUSIONS

The methodology proposed for the simulation of biomechanical models subjected to impact loading shows a good aptitude to describe the results necessary to fully analyse the human body motion. The relative motion between the body segments is kept within feasible regions by applying penalty torques in the joints when the limits of the relative motion are reached. Among the results obtained with this model, the reaction forces between the biomechanical segments are fully available. Further improvements can be obtained with a more detailed description of the biomechanical joints. Though not considered here, the model proposed allows for the description of the muscle actions, that may play a role during less severe impacts. Another aspect that plays an important role in some impact conditions is the kinematics of the head-neck and spine. A more detailed description of the upper torso using flexible bodies may be important to obtain more credible results. The contact between body and surrounding objects is efficiently modelled by a continuous contact force model that includes energy dissipation due to local deformations. However, for an effective use of this model, it is necessary a characterisation of the surfaces in contact. Applications to the study of a car occupant and of a player subjected to a tackle describe the use of the methodology.

AKNOWLEDGEMENTS

REFERENCES

Bayo, E., Ledesma, R. (1996). Augmented Lagrangean and mass-orthogonal projection methods for constrained multibody dynamics, Nonlinear Dynamics, 9 (1-2), 113-130.

Berme, N., Heydinger, G., Capozzo, A. (1978) Calculation of loads transmitted at the anatomical joints, Biomechanics of engineering modelling, simulation, control (A. Morecki Ed), Heidelberg, Germany; Springer-Verlag 89-131

CIBA GEIGY, (1979). Folia Rheumatologica, Motilität von Hüfte, Schulter, Hand und Fuβ, GrubH Wehr/Baden.

Hertz, H. (1895). Gesammelte Werke, 1, Leipzig, Germany.

Haug, E.J. (1989). Computer-aided kinematics and dynamics of mechanical systems, vol I: basic methods, Boston, Massachusetts: Allyn & Bacon.

Jalón, J.G. (1994). Kinematic and dynamic simulation of multibody systems, Heidelberg: Springer-Verlag.

Jerkovsky, W. (1978). The structure of multibody dynamic equations, Journal of Guidance and Control, 1, 173-182.

Kane, T.R., Levinson, D.A. (1985). Dynamics: theory and applications, New York, New York: McGraw-Hill.

Laananen, D. (1983). Computer Simulation of an aircraft seat and occupant in a crash environment - Vol. 1: Technical report, US Dep. of Transportation, F.A.A., Technical Report DOT/FAA/CT-82/33-I.

Lankarani, H., Nikravesh, P.E. (1990). A contact force model with hysteresis damping for impact analysis of multibody systems, ASME Journal of Mechanical Design, 112, 369-376.

Lankarani, H., Nikravesh, P.E. (1992). Canonical impulse-momentum equations for the impact analysis of mult5body systems, ASME Journal of Mechanical Design, 114, 180-186.

Lankarani, H., Ma, D., Menon, R. (1995). Impact dynamics of multibody mechanical systems and application to crash responses of aircraft occupant/structure. Computational Dynamics in Multibody Systems, (eds. M.Pereira e J.Ambrósio) Dordrecht, Netherlands: Kluwer. 239-265.

Nigg, B.M., Herzog, W. (1994). Biomechanics of the musculo-skeletal system, Toronto, Canada: John Wiley & Sons.

Nikravesh, P.E. (1988). Computer-aided analysis of mechanical systems. Englewood-Cliffs, New Jersey: Prentice-Hall.

Nikravesh, P.E., Gim, G. (1989). Systematic construction of the equations of motion for multibody systems containing closed kinematic loops. ASME Advances in Design Automation, 3, 27-33.

Pereira, M.S., Ambrósio, J.A.C. (1994) Computer-aided analysis of rigid and flexible mechanical systems, Dordrecht, Netherlands; Kluwer.

Silva, M.S.T, Ambrósio, J.A.C. (1996). Modelo biomecânico para a dinâmica computacional do movimento humano articulado (Biomechanical model for the computational dynamics of the human articulated motion), Technical Report IDMEC/CPM-96/003, IDMEC - Instituto Superior Técnico.

Winter, D.A. (1990). Biomechanics and motor control of human movement, Toronto; John Wiley & Sons.